

Magnetic field induced dehybridization of the electromagnons in multiferroic TbMnO₃

P. Rovillain¹, M. Cazayous¹, Y. Gallais¹, M-A. Measson¹, A. Sacuto¹, H. Sakata², and M. Mochizuki³

¹*Laboratoire Matériaux et Phénomènes Quantiques (UMR 7162 CNRS),*

Université Paris Diderot-Paris 7, 75205 Paris cedex 13, France

²*Department of Physics, Tokyo University of Science,*

1-3 Kagurazaka Shinjyuku-ku Tokyo 162-8601, Japan

³*Department of Applied Physics, The University of Tokyo,*

7-3-1, Hongo, Bunkyo-ku, Tokyo 113-8656, Japan

We have studied the impact of the magnetic field on the electromagnon excitations in TbMnO₃ crystal. Applying magnetic field along the c axis, we show that the electromagnons transform into pure antiferromagnetic modes, losing their polar character. Entering in the paraelectric phase, we are able to track the spectral weight transfer from the electromagnons to the magnon excitations and we discuss the magnetic excitations underlying the electromagnons. We also point out the phonons involved in the phase transition process. This reveals that the Mn-O distance plays a key role in understanding the ferroelectricity and the polar character of the electromagnons. Magnetic field measurements along the b axis allow us to detect a new electromagnon resonance in agreement with a Heisenberg model.

PACS numbers:

Ferroelectric order is unlikely to be present in magnetic compounds. The coexistence of magnetism and ferroelectricity is so rare that the rediscovery of materials combining both properties in the so-called multiferroic materials has given rise to a strong revival of this field. In multiferroics, the coupling between the magnetic and ferroelectric orders represents a promising route to the electrical control of magnetic properties for storage and for processing devices[1–3]. Some multiferroics not only present a simple phase coexistence between both orders but a ferroelectricity induced by the magnetic structure. This is the case for perovskite manganites RMnO₃ (R=Rare earth) in which the spiral spin structure breaks the inversion symmetry of the magnetic ordering and gives rise to a ferroelectric state. A purely electronic mechanism or a magnetically induced ionic displacement mechanism based on the Dzyaloshinskii-Moriya coupling have both been proposed for the origin of this ferroelectricity [4, 5]. Such mechanisms explain the static properties of perovskites but fail in the interpretation of the dynamical coupling between spin and charge degrees of freedom. The mixing of spin waves (magnons) with optical phonons creates a novel class of excitations called electromagnons, magnons with a dipolar activity. These electromagnon excitations were recently interpreted using microscopic approaches based on Heisenberg interaction [6] and taking into account the ground state spin spiral configuration [7, 8].

TbMnO₃ is the most representative compound of this class of multiferroics. In its antiferromagnetic phase ($T_N = 41$ K), a sinusoidal spin structure is replaced by a cycloid magnetic order below 28 K breaking the inversion symmetry of the crystal and inducing a spontaneous polarization along the c axis. In this phase, the spins form a spiral with an incommensurate wavevector $\mathbf{Q}_b = (0, 0.28, 0)$ in the bc plane. The spin-spiral plane can flip from the bc into the ab plane with an external magnetic field along

the a and b axis. Two electromagnons have been measured by infrared (IR) [9, 10], terahertz (THz) [11] and Raman [12] spectroscopies and by inelastic neutron scattering [13]. Both electromagnons are always optically excited using an electric field of the light parallel to the a axis irrespective of the spiral-plane orientation (bc or ab). This specific selection rule shows that electromagnons are tied to the lattice rather than the spin structure [6]. However, the structural origin of the polar activity of the electromagnons has not been yet identified.

In this letter, we show that the electric dipole character of the electromagnons disappears and their pure magnetic part emerges when the spin spiral is destabilized with a magnetic field along the c axis. The spectral weight transfer from the electromagnons to the magnon excitations sheds light on the magnetic excitations involved in the formation of electromagnons. The effect of the phase transitions on the phonon modes shows that the Mn-O distance is the crucial length for understanding the ferroelectricity and the polar character of the electromagnons. The phase diagram for a magnetic field along the b axis is also explored and a new electromagnon resonance is observed in agreement with calculations from a Heisenberg model.

Single $Pbnm$ crystals of TbMnO₃ were grown by the floating-zone method and oriented by Laue x-ray diffraction. Two samples were investigated : (i) an ab and (ii) an ac sample for magnetic field along the c and b axis, respectively. We have performed Raman measurements in a backscattering geometry with a triple spectrometer Jobin Yvon T64000 using the 568 nm excitation line from a Ar⁺-Kr⁺ mixed gas laser [12].

Figure 1a shows the magnetoelectric phase diagram of TbMnO₃ for \mathbf{B}/c [14–16]. Previous transport measurements have shown that the spontaneous polarization is rapidly suppressed above 8 T and TbMnO₃ becomes

paraelectric [14]. Additional neutron measurements show that the incommensurate magnetic structure is destabilized between 7 and 10 T [15]. Above 10 T, TbMnO_3 becomes a simple A-type antiferromagnetic [15].

Figure 1c shows at zero magnetic field the two electromagnons modes ($e_1 \approx 30 \text{ cm}^{-1}$ and $e_2 \approx 60 \text{ cm}^{-1}$) measured on the ab TbMnO_3 sample. The electric field of light \mathbf{E}^ω of the incident and scattered photons are parallel to the a axis. These excitations disappear above the Curie temperature indicating their electromagnon origin [12]. In addition THz measurements have detected electromagnons in the same energy ranges and with the same polarization $\mathbf{E}^\omega // a$ further reinforcing this assignment [18]. The e_1 electromagnon is observed in IR and THz at lower energy around $20\text{--}25 \text{ cm}^{-1}$ which is identical to the energy of the antiferromagnetic resonance (AFMR). These excitations can be distinguished only by their optical selection rules [9]. IR and THz measurements lead to the interpretation of the one magnon (AFMR) labeled 1M in Fig. 1b as the magnetic part of the e_1 electromagnon. However, recent theoretical approaches predict different energies for the AFMR and the e_1 electromagnon (see the dispersion curve in the spiral spin state of Fig. 1b) [7, 8]. Based on calculations of Refs. 7 and 8, the wavevectors of the e_1 and e_2 electromagnons should be equal to $q_{e_1} = \pi - 2Q_b$ ($Q_b = 0.28$ is the magnitude of the cycloidal wavevector) and $q_{e_2} = \pi$ (zone-edge electromagnon) in the dispersion of the spin spiral AFM state (see Fig. 1b). This dispersion corresponds to the spin oscillations out of the bc spiral plane rotating around the c axis [13]. Given these discrepancies, it is fundamental to experimentally determine the magnetic excitation associated to the e_1 electromagnon in order to find the mechanism at the origin of the electromagnons. The investigation of the TbMnO_3 phase diagram when a magnetic field \mathbf{B} is applied along the c axis gives the opportunity to shed light on this question.

Figure 1c and d present the Raman spectra along path 1 ($T = 10 \text{ K}$ in Fig. 1a). The frequency of the e_1 and e_2 electromagnons (Fig. 1c) respectively decreases and increases with the magnetic field. For $B = 8 \text{ T}$, one sharp peak appears at 21 cm^{-1} (1M) in Fig. 1c and two broader peaks at 88 cm^{-1} ($2M_{\text{spiral}}^1$, Fig. 1c) and 140 cm^{-1} ($2M_{\text{spiral}}^2$) in Fig. 1d. At the same time, the electromagnons intensity is drastically reduced and disappears at $B = 10 \text{ T}$.

The additional peaks measured above 8 T in the paraelectric phase are associated to magnetic excitations. Simple Tb^{3+} f-f transitions have different energies and can be ruled out [19]. The 1M peak corresponds to the zone center magnon of the magnon dispersion in the spin spiral state (see Fig. 1b). The $2M_{\text{spiral}}^1$ and $2M_{\text{spiral}}^2$ peaks are associated to two-magnon excitations. The two-magnon excitation is formed from two zone-edge magnons with opposite wavevectors. The energies of

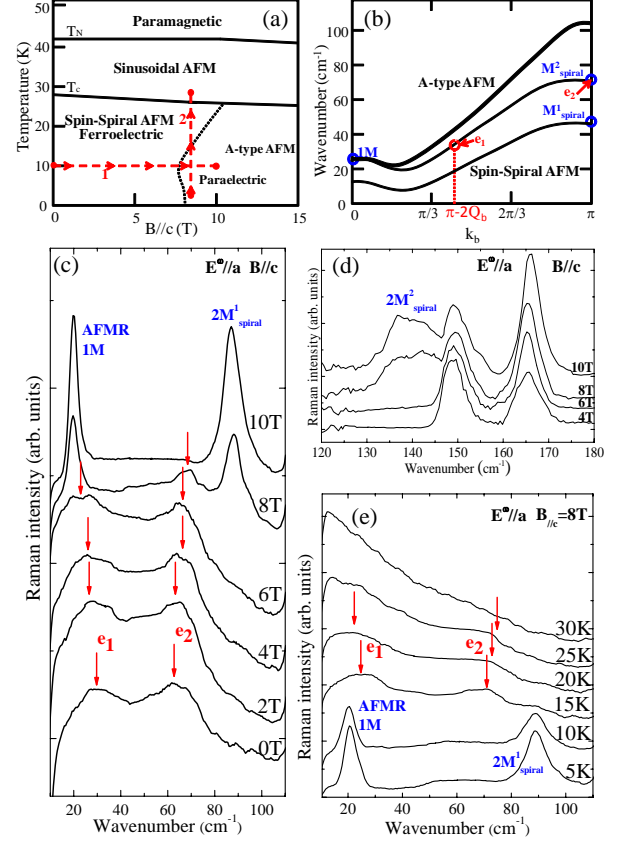


FIG. 1: (a) Magnetoelectric phase diagram of TbMnO_3 with $\mathbf{B} // c$. (b) Magnon dispersions along $\mathbf{k} = (0, k_b, 0)$. The two lower magnon dispersions in the spin-spiral AFM state are extracted from neutron measurements [20]. The upper (bold) magnon dispersions have been calculated in the A-type AFM state. The center 1M, M_{spiral}^1 and M_{spiral}^2 correspond to the zone center magnon and to the zone-edge magnon modes in the spin-spiral state, respectively. e_1 is the predicted electromagnon with a wavevector equal to $\pi - 2Q_b$ and e_2 the electromagnon at the zone edge of the Brillouin zone. (c-d) Raman spectra obtained with $\mathbf{E}^\omega // a$ and $\mathbf{B} // c$ along the path 1 (see (a)). (e) Raman spectra obtained increasing temperature along the path 2 (see (a)). Arrows indicate the e_1 and e_2 modes. One can notice that the Tb crystal field at 4.5 meV (36 cm^{-1}) is not observed.[13]

$2M_{\text{spiral}}^1$ and $2M_{\text{spiral}}^2$ two-magnons are twice the M_{spiral}^1 and M_{spiral}^2 zone edge energies of the magnon dispersions in the spin spiral state (see Fig. 1b). The energies of these modes are in agreement with neutron measurements [20].

From these observations, one can deduce that the spin structure associated with the spiral spin state survives above 8 T. A magnetic field above 10 T should swing TbMnO_3 to a pure A-type antiferromagnetic phase [15] and the two-magnon excitation of the zone-edge A-type AFM dispersion should be measured around 200 cm^{-1} (see Fig. 1b). This peak is not experimentally detected up to 10 T. The A-type AFM phase was not observed here. The 8-10 T range might be interpreted as a hystere-

sis region of the first-order phase transition. Entering in the paraelectric phase, the electromagnons e_1 and e_2 disappear quickly whereas the intensity of the one-magnon ($1M$) and two-magnon excitations ($2M_{spiral}^1$ and $2M_{spiral}^2$ peaks) drastically increase. There is a clear difference between the magnon modes and the electromagnons. Both excitations do not have the same energy and nor the same width. Moreover, there is a clear spectral weight transfer from electromagnons to pure magnon excitations entering the paraelectric phase (see Fig. 1c). We can notice that the energy of an excitation at $\pi-2Q_b$ in the spin spiral AFM dispersion of Fig. 1b is around 30 cm^{-1} and the one magnon excitation has an energy around 20 cm^{-1} as experimentally observed in Raman measurements. This difference suggests that the e_1 electromagnon observed using Raman scattering is associated with a magnetic excitation at $k=\pi-2Q_b$ and not at $k=0$.

According to Refs. 7 and 8 the e_2 electromagnon is Raman active due to the folding of the Brillouin zone. The periodicity of the lattice is doubled and the originally $q_{e2}=(0,\pi,0)$ electromagnon becomes an excitation at the Gamma ($k=0$) point. For the lower energy electromagnon at $q_{e1}=(0,\pi-2Q_b,0)$, the Brillouin zone is folded at the wave vector equal to Q_b due to the spiral magnetic structure. Then the e_1 electromagnon also becomes an excitation at the Gamma point.

Figure 1e shows the Raman spectra obtained by increasing the temperature along path 2 ($B=8 \text{ T}$) in Fig. 1a. The AFMR and the $2M_{spiral}^1$ peaks disappear between 10K and 15K (the $2M_{spiral}^2$ is not shown here but it disappears in the same temperature range). In the same range of temperatures, the e_1 and e_2 electromagnon peaks are emerging and then disappear above 25 K. These observations are in agreement with the reported phase diagram (Fig. 1a). It confirms that the electromagnons exist only in the ferroelectric phase and that the pure magnetic excitations exist only in the paraelectric phase.

From the structural point of view, IR measurements have suggested that the Mn atomic displacement is mainly at the origin of the ferroelectricity induced by the Dzyaloshinskii-Moriya interaction [21]. For the polar part of the electromagnons, the spectral weight transfer observed in IR from phonons to the electromagnons shows that their polar activity mainly comes from phonons [10, 21, 22]. However the exact structural origin of the ferroelectricity and the origin of the electromagnon polar activity are not determined.

Figure 2a and b show the phonon spectra for zero and 10 T along the c axis using cross xy (B_{1g}) and parallel xx (A_g) polarizations of light, respectively. Over the 7 A_g and 7 B_{1g} Raman active modes predicted by the group theory, all the modes have been detected and assigned in agreement with previous measurements [23, 24]. The new modes have been assigned by comparison with simulations [25]. A magnetic field along the a and b axis

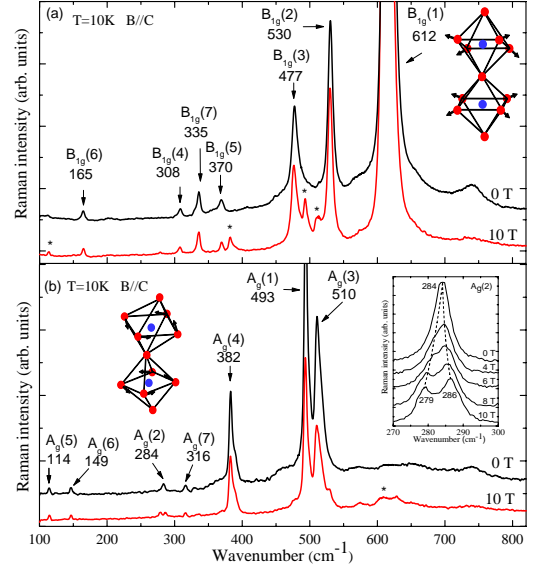


FIG. 2: Raman spectra of phonon modes for 0 and 10 T in cross xx (a) and parallel xx (b) polarization of light. Raman spectra in cross polarization shows 7 B_{1g} modes (a) and 7 A_g modes (b) in parallel polarization at 0 T. The insert in (b) show the splitting of $A_g(2)$ phonon mode (MnO_6 block rotation) with the magnetic field. The A_g modes are obtained in $z(xx)\bar{z}$ geometry with eigenvectors parallel to the x direction. The B_{1g} modes are obtained in $z(xy)\bar{z}$ geometry with eigenvectors parallel to the x and y directions. Stars indicate phonon modes due to polarization leakage.

induces a linear shift of phonon frequencies of less than 0.5 cm^{-1} . With a magnetic field along c , two phonon modes depart from this simple behavior: the frequency of $B_{1g}(1)$ mode shifts of 2 cm^{-1} and the $A_g(2)$ mode splits into two peaks (inset of Fig. 2b).

The $A_g(2)$ phonon mode is associated to the rotation of the MnO_6 block around the y axis (cubic notations) (see Fig. 2b). The $A_g(2)$ phonon mode frequency is linearly proportional to the MnO_6 block rotation angle by a factor of $23.5 \text{ cm}^{-1}/\text{deg}$ [24]. The splitting of the $A_g(2)$ peak (284 cm^{-1}) into the 279 and 286 cm^{-1} peaks is equivalent to the rotation of the MnO_6 block by -0.2° and $+0.08^\circ$, respectively. Moreover, the MnO_6 block rotation α is connected to variation of the oxygen atom position: $\alpha = \arctan(2|(x_0 - z_0)|)$. The measured rotation of the MnO_6 block can be associated with the variation of the oxygen atom position $x_0 - z_0$ by about 1.5% from its initial position. We note that the symmetry of the paraelectric phase is higher than the ferroelectric one and less Raman modes are expected in the paraelectric phase. However, TbMnO_3 is not a standard ferroelectric and this unusual behaviour has been already pointed out [21].

The $B_{1g}(1)$ mode corresponds to the in-plane oxygen stretching vibration in the xz plane and is determined by the Mn-O distance. This mode is the so called Jahn-

Teller mode. The frequency of the $B_{1g}(1)$ mode is proportional to $d_{Mn-O}^{3/2}$. The frequency shift of the $B_{1g}(1)$ peak corresponds to an increase of 0.1% of the Mn-O distance (the Mn-O distance is equal to 2.063 Å in $TbMnO_3$ at zero field). Pure electronic or magnetically induced ionic displacement mechanisms have been proposed for the origin of the ferroelectric polarization. From an experimental point of view, no phonon anomaly has been detected by inelastic neutron scattering supporting the electronic origin of the ferroelectricity [26]. Previously, only IR measurements have been able to detect a small phonon softening (0.5 cm^{-1}) at the ferroelectric transition [21]. Only with the magnetic field along the c -axis, a strong renormalization of two phonons frequency can be measured when $TbMnO_3$ becomes paraelectric and the electric activity of the electromagnons vanishes with a 8 T magnetic field. Based on these observations, we suggest that the ferroelectricity and the polar activity of the electromagnon are related to the change of the oxygen atom position and correlated with the increase of the Mn-O distance.

We have also performed magnetic measurements along the b axis. Figure 3a shows the Raman spectra measured on the ac $TbMnO_3$ sample excited by an electric field of light $\mathbf{E}^\omega//a$ and with a magnetic field B along the b axis. Increasing B from 0 to 4 T, the Raman spectra remain unchanged. Above 4 T, the frequency of the e_1 and e_2 electromagnons is weakly shifted. An additional peak appears at 4 T around 78 cm^{-1} when the spin spiral flips from the bc to the ab plane and shifts down to 68 cm^{-1} at 10 T. Figure 3b compares the calculated spectral weight of electromagnons for a magnetic field $B=0\text{ T}$ (bc spiral plane) and $B=8\text{ T}$ (ab spiral plane). The calculations are performed in the same way as in Ref. 8 using a system with $20\times 20\times 6$ sites. The model parameters for $TbMnO_3$ can be found in Ref. 17. A peak shows up clearly around 90 cm^{-1} for $B=8\text{ T}$ when the spin spiral flips in the ab plane. It comes from the exchange and easy-plane anisotropy terms. The splitting is caused by the spin-structure modulation induced by the applied magnetic field. Based on the Heisenberg model, this additional peak is interpreted as an electromagnon resonance.

In summary, our measurements show the dehybridization of the electromagnons with a magnetic field along c and reveal the spectral weight transfer from the electromagnons to the magnon modes. The phonon modes are also strongly impacted. The Mn-O distance appears as the crucial parameter to understand the ferroelectricity and the polar activity of the electromagnons.

The authors would like to thank R. P. S. M. Lobo for helpful discussions.

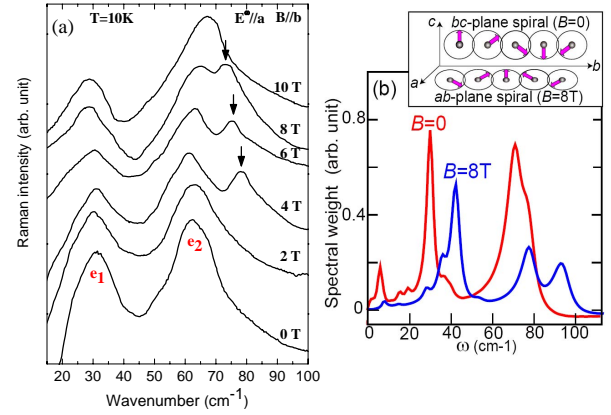


FIG. 3: (a) Magnetic field dependence ($B//b$) of Raman spectra for a polarization of light $\mathbf{E}^\omega//a$. Two electromagnon modes e_1 and e_2 are measured at 30 cm^{-1} and 60 cm^{-1} , respectively. An additional peak appears at 4 T around 78 cm^{-1} when the spiral spin flips from the bc to the ab plane. (b) Sketch of the magnetic spiral structure and calculated spectral weight of electromagnons at $B=0\text{ T}$ (bc spiral plane) and $B=8\text{ T}$ (ab spiral plane).

-
- [1] W. Eerenstein, N. D. Mathur, and J. F. Scott, *Nature* **442**, 759 (2006).
 - [2] Y.-H. Chu, *et al.* *Nature Mater.* **7**, 478 (2008).
 - [3] S. H. Baek, *et al.* *Nature Mater.* **9**, 309 (2010).
 - [4] H. Katsura, N. Nagaosa, and A. V. Balatsky, *Phys. Rev. Lett.* **95**, 057205 (2005).
 - [5] I. A. Sergienko, and E. Dagotto, *Phys. Rev. B* **73**, 094434 (2006).
 - [6] R. Valdés Aguilar *et al.*, *Phys. Rev. Lett.* **102**, 047203 (2009).
 - [7] M.P.V. Stenberg, and R. de Sousa, *Phys. Rev. B* **80**, 094419 (2009).
 - [8] M. Mochizuki, N. Furukawa, and N. Nagaosa, *Phys. Rev. Lett.* **104**, 177206 (2010).
 - [9] A. B. Sushkov, R. V. Aguilar, S. Park, S.-W. Cheong, and H. D. Drew, *Phys. Rev. Lett.* **98**, 027202 (2007).
 - [10] Y. Takahashi *et al.*, *Phys. Rev. Lett.* **101**, 187201 (2008).
 - [11] A. Pimenov *et al.*, *Nature Physics* **2**, 97 (2006).
 - [12] P. Rovillain, M. Cazayous, Y. Gallais, A. Sacuto, M.-A. Measson, and H. Sakata, *Phys. Rev. B* **81**, 054428 (2010).
 - [13] D. Senff *et al.*, *Phys. Rev. Lett.* **98**, 137206 (2007).
 - [14] T. Kimura, G. Lawes, T. Goto, Y. Tokura, and A. P. Ramirez, *Phys. Rev. B* **71**, 224425 (2005).
 - [15] D. N. Argyriou *et al.*, *Phys. Rev. B* **75**, 020101(R) (2007).
 - [16] M. Mochizuki, and N. Furukawa, *Phys. Rev. Lett.* **105**, 187601 (2010).
 - [17] A. Pimenov, A. M. Shuvaev, A. A. Mukhin and A. Loidl, *J. Phys.: Condens. Matter* **20**, 434209 (2008).
 - [18] A. Pimenov *et al.*, *Phys. Rev. Lett.* **102**, 107203 (2009).
 - [19] J. A. Koningstein, and G. Schaack, *Phys. Rev. B* **2**, 1242 (1970); D. Boal *et al.*, *Phys. Rev. B* **7**, 4757 (1973); V. V. Eremin *et al.*, *Low. Temp. Phys.* **33**, 915 (2007).
 - [20] D. Senff *et al.*, *J. Phys.: Condens. Matter* **20**, 434212 (2008).

- [21] R. Schleck, R. L. Moreira, H. Sakata, and R. P. S. M. Lobo, Phys. Rev. B **82**, 144309 (2010).
- [22] A. Pimenov, *et al.*, Phys. Rev. B **74**, 100403(R) (2006).
- [23] J. Laverdière *et al.*, Phys. Rev. B **73**, 214301 (2006).
- [24] M. N. Iliev *et al.*, Phys. Rev. B **73**, 064302 (2006).
- [25] R. Choithrani, M. N. Rao, S. L. Chaplot, N. K. Gaur, and R. K. Singh, arXiv:1004.0634.
- [26] R. Kajimoto *et al.*, Phys. Rev. Lett. **102**, 247602 (2009).